

# Optimal Superconvergence of Energy Conserving Local Discontinuous Galerkin Methods for Wave Equations

Waixiang Cao<sup>1</sup>, Dongfang Li<sup>2,3,\*</sup> and Zhimin Zhang<sup>1,4</sup>

<sup>1</sup> Beijing Computational Science Research Center, Beijing 100193, China.

<sup>2</sup> School of Mathematics and Statistics, Huazhong University of Science and Technology, Wuhan 430074, China.

<sup>3</sup> Department of Mathematics, City University of Hong Kong, Kowloon, Hong Kong.

<sup>4</sup> Department of Mathematics, Wayne State University, Detroit, MI 48202, USA.

Communicated by Chi-Wang Shu

Received 12 July 2015; Accepted (in revised version) 10 May 2016

---

**Abstract.** This paper is concerned with numerical solutions of the LDG method for 1D wave equations. Superconvergence and energy conserving properties have been studied. We first study the superconvergence phenomenon for linear problems when alternating fluxes are used. We prove that, under some proper initial discretization, the numerical trace of the LDG approximation at nodes, as well as the cell average, converge with an order  $2k+1$ . In addition, we establish  $k+2$ -th order and  $k+1$ -th order superconvergence rates for the function value error and the derivative error at Radau points, respectively. As a byproduct, we prove that the LDG solution is superconvergent with an order  $k+2$  towards the Radau projection of the exact solution. Numerical experiments demonstrate that in most cases, our error estimates are optimal, i.e., the error bounds are sharp. In the second part, we propose a fully discrete numerical scheme that conserves the discrete energy. Due to the energy conserving property, after long time integration, our method still stays accurate when applied to nonlinear Klein-Gordon and Sine-Gordon equations.

**AMS subject classifications:** 65L20, 65M12, 65N12

**Key words:** Local discontinuous Galerkin methods (LDG), wave equations, superconvergence, energy conserving.

---

## 1 Introduction

We study the local discontinuous Galerkin (LDG) method for the following 1D wave equations

---

\*Corresponding author. *Email addresses:* wxcao@csrcc.ac.cn (W. Cao), dfli@hust.edu.cn (D. Li), zmzhang@csrcc.ac.cn, zzhang@math.wayne.edu (Z. Zhang)

$$\begin{aligned} u_{tt} &= u_{xx} + f(u), & (x, t) \in [a, b] \times [0, T], \\ u(x, 0) &= u_0(x), & u_t(x, 0) = u_1(x) \end{aligned} \quad (1.1)$$

with the periodic boundary condition. We investigate superconvergence property of the LDG method for the linear problem, and an energy conserving fully discrete scheme for the nonlinear problem.

The superconvergence of DG, especially LDG methods has been one of the hot research spots in recent years. We refer to [1, 2, 7, 16, 22, 24, 28] for the investigation related to ordinary and delay differential equations, [3, 8, 11, 26] for hyperbolic equations and [9, 12, 21, 27] for convection-diffusion equations. Superconvergence of the LDG method for wave equations has also been investigated. In particular, Baccouch proved a local superconvergence rate of  $k+2$  and a global superconvergence rate of  $k+3/2$  at Radau points for 1D wave equations [5] and [6]. Xing et al. presented an energy conserving LDG method for wave propagation and also proved a  $k+3/2$ -th superconvergence rate of the LDG approximation to a special projection of the exact solution [25]. However, numerical experiments for wave equations indicated that aforementioned theoretical rates were not sharp. In order to establish the optimal superconvergence results for LDG methods, some new analysis tools were developed very recently. The main idea was to construct, in the discrete space, a special function, which was used to correct the error between the LDG solution and the Gauss-Radau projection of the exact solution. Thanks to the correction function, we established the optimal superconvergence rate of the LDG method for the hyperbolic problems [8] and parabolic problems [9], respectively. Now, we try to complete the jigsaw puzzle and continue the study of the optimal superconvergence results for wave equations.

The first part of this paper is to revisit superconvergence properties of the LDG method for wave equations. We provide a rigorous mathematical proof of the optimal superconvergence rate for the LDG method. On one hand, for the first time we show that the numerical trace of the LDG approximation at nodes, as well as the cell average, is superconvergent with the order  $2k+1$ . On the other hand, the function value approximation and the derivative approximation are superconvergent with orders  $k+2$  and  $k+1$  at Radau points, respectively. The superconvergence results at the Radau points improve these in [6] and [25]. As a byproduct, a  $k+2$ -th superconvergence order of the LDG solution towards a particular Gauss-Radau projection of the exact solution is obtained. Moreover, our analysis also leads to some interesting numerical discoveries, which will be reported in the numerical experiments.

The analysis of this paper is based on the correction function idea, which is motivated from its successful application to hyperbolic [8] and parabolic equations [9]. But the construction of the correct functions for wave equations is more technical and complicated. It is different from the DG method for hyperbolic equations [8] due to the interplay between two correction functions. We have to rewrite the wave equation as a system of first order partial differential equations with respect to the spacial variable  $x$ . The correction

functions for both variables (the exact solution  $u$  and an auxiliary variable  $q = u_x$ ) have to be constructed simultaneously. The construction is also different from the LDG method for parabolic problems [9] due to the second order time derivative and the source linear term.

The second part is devoted to developing a fully discrete numerical scheme that conserves the discrete energy of the nonlinear wave equation. As is well-known, many numerical schemes are developed to achieve the energy conserving property of wave equations, such as the finite difference method [17, 19], spectral element method [4, 18], DG method [13–15, 23]. However, very few explicit time marching algorithms on unstructured grids can preserve energy for nonlinear wave equations. In this study, the LDG method is used on an unstructured grid for the spatial variable, and the time discretization is achieved by an explicit multi-step method. With a special treatment of the nonlinear term, we prove the energy conservation property of the fully discrete scheme. Numerical tests reveal that without the special treatment of the nonlinear term, the algorithm may result in substantial phase and shape errors after a long time integration.

The rest of the paper is organized as follows. In Section 2, we present a semi-discrete LDG method for (1.1) when alternating fluxes are used. In Section 3, we first introduce some preliminaries and then construct special correction functions and interpolation functions. With the specially designed correction functions, we provide superconvergence results for the linear viscous wave equations. In Section 4, we present a fully discrete energy conserving LDG schemes for (1.1). Finally, numerical illustrations are presented in Section 5 and future works and concluding remarks are presented in Section 6, respectively.

Throughout this paper, we use the standard notations for Sobolev spaces such as  $W^{m,p}(D)$  on sub-domain  $D \subset \Omega$  equipped with the norm  $\|\cdot\|_{m,p,D}$  and semi-norm  $|\cdot|_{m,p,D}$ . When  $D = \Omega$ , we omit the index  $D$ ; if  $p = 2$ , we set  $W^{m,p}(D) = H^m(D)$ ,  $\|\cdot\|_{m,p,D} = \|\cdot\|_{m,D}$  and  $|\cdot|_{m,p,D} = |\cdot|_{m,D}$ .

## 2 Local discontinuous Galerkin spatial discretization

For the spatial discretization of the one-dimensional problem (1.1), we divide the domain  $\Omega = [a, b]$  with a mesh:  $a = x_{\frac{1}{2}} < x_{\frac{3}{2}} < \dots < x_{N+\frac{1}{2}} = b$  and denote the intervals by  $\tau_j = (x_{j-\frac{1}{2}}, x_{j+\frac{1}{2}})$ . Let  $h_j = x_{j+\frac{1}{2}} - x_{j-\frac{1}{2}}$ ,  $\bar{h}_j = h_j/2$  and  $h = \max_{1 \leq j \leq N} h_j$ , and suppose the mesh is quasi-uniform. Define a  $k$ -degree discontinuous finite element space

$$V_h = \{v: v|_{\tau_j} \in \mathbb{P}^k(\tau_j), j \in \mathbb{Z}_N\},$$

where  $\mathbb{P}^k(\tau_j)$  denotes the set of all polynomials of degree no more than  $k$  on  $\tau_j$ , and  $\mathbb{Z}_r = \{1, 2, \dots, r\}$  for any positive integer  $r$ . Here and below, to simplify the notation, we will make the following substitutions if needed

$$v(x, t) = v(t) = v,$$

where  $v = u, u_h, q, q_h$ . We also denote by  $v_{j-\frac{1}{2}}^+ = v(x_{j-\frac{1}{2}}^+, t)$  and  $v_{j-\frac{1}{2}}^- = v(x_{j-\frac{1}{2}}^-, t)$  the right and left limits of the discontinuous function  $v$  at the boundary point  $x_{j-\frac{1}{2}}$ , respectively.

To obtain the LDG scheme, we first rewrite (1.1) as

$$u_{tt} - q_x = f(u), \quad q - u_x = 0. \quad (2.1)$$

The semi-discrete LDG method is to find  $u_h, q_h \in V_h$ , such that, for all test functions  $v, p \in V_h$  and  $1 \leq j \leq N$ ,

$$((u_h)_{tt} - f(u_h), v)_j + (q_h, v_x)_j - \hat{q}_h v^-|_{j+\frac{1}{2}} + \hat{q}_h v^+|_{j-\frac{1}{2}} = 0, \quad (2.2)$$

$$(q_h, p)_j + (u_h, p_x)_j - \hat{u}_h p^-|_{j+\frac{1}{2}} + \hat{u}_h p^+|_{j-\frac{1}{2}} = 0, \quad (2.3)$$

where  $(u, v)_j = \int_{\tau_j} u v dx$  and  $\hat{q}_h, \hat{u}_h$  are the numerical fluxes. These fluxes, which in general are dependent on the values of the discontinuous numerical solution from both sides, play an important role in assuring numerical stability of the method. In this paper, we consider the alternating fluxes:

$$\hat{q}_h = q_h^+, \quad \hat{u}_h = u_h^-, \quad (2.4)$$

or

$$\hat{q}_h = q_h^-, \quad \hat{u}_h = u_h^+. \quad (2.5)$$

### 3 Superconvergence of the LDG method for the linear case

This section is devoted to the superconvergence of the LDG method for the linear wave equation, i.e., we consider Eq. (1.1) with

$$f(u) = \alpha u,$$

where  $\alpha$  is a constant.

#### 3.1 Preliminaries

We first define

$$\mathcal{D}(\xi, \eta; \hat{\xi}) = \sum_{j=1}^N \mathcal{D}_j(\xi, \eta; \hat{\xi}),$$

where

$$\mathcal{D}_j(\xi, \eta; \hat{\xi}) = (\xi, \eta_x)_j - \hat{\xi} \eta^-|_{j+\frac{1}{2}} + \hat{\xi} \eta^+|_{j-\frac{1}{2}}.$$

Then the LDG schemes (2.2)-(2.3) can be rewritten as

$$((u_h)_{tt} - \alpha u_h, v)_j + \mathcal{D}_j(q_h, v; \hat{q}_h) = 0, \quad (q_h, p)_j + \mathcal{D}_j(u_h, p; \hat{u}_h) = 0, \quad \forall v, p \in V_h. \quad (3.1)$$

Taking the time derivative of the second equation of (3.1) yields

$$((q_h)_t, p)_j + \mathcal{D}_j((u_h)_t, p; (\hat{u}_h)_t) = 0.$$

Hence, by denoting

$$\mathcal{A}_j(\xi, \eta; v, p) = (\xi_{tt} - \alpha \xi, v)_j + \mathcal{D}_j(\eta, v; \hat{\eta}) + (\eta_t, p)_j + \mathcal{D}_j(\xi_t, p; (\hat{\xi})_t)$$

and

$$\mathcal{A}(\xi, \eta; v, p) = \sum_{j=1}^N \mathcal{A}_j(\xi, \eta; v, p),$$

where  $(\hat{\xi}, \hat{\eta})$  are taken as the alternating fluxes (2.4) or (2.5), we obtain

$$\mathcal{A}(u_h, q_h; v, p) = 0, \quad \forall v, p \in V_h.$$

Obviously, the exact solutions  $u, q$  also satisfy

$$\mathcal{A}(u, q; v, p) = 0, \quad \forall v, p \in V_h.$$

Let

$$H_h^1 = \{v : v|_{\tau_j} \in H^1(\tau_j), j \in \mathbb{Z}_N\},$$

and for any given function  $v \in H_h^1$ , we define two special projections  $P_h^- v, P_h^+ v$  as follows:

$$\begin{aligned} (P_h^- v, w)_j &= (v, w)_j, \quad \forall w \in \mathbb{P}^{k-1}(\tau_j) \quad \text{and} \quad P_h^- v(x_{j+\frac{1}{2}}^-) = v(x_{j+\frac{1}{2}}^-), \\ (P_h^+ v, w)_j &= (v, w)_j, \quad \forall w \in \mathbb{P}^{k-1}(\tau_j) \quad \text{and} \quad P_h^+ v(x_{j-\frac{1}{2}}^+) = v(x_{j-\frac{1}{2}}^+). \end{aligned}$$

Note that the two projection operators are commonly used in the analysis of DG methods.

For any function  $v \in H_h^1$ , we have the following Legendre expansion in each element  $\tau_j, j \in \mathbb{Z}_N$ ,

$$v(x) = \sum_{m=0}^{\infty} v_{j,m} L_{j,m}(x), \quad v_{j,m} = \frac{2m+1}{h_j} (v, L_{j,m})_j,$$

where  $L_{j,m}$  denotes the normalized Legendre polynomial of degree  $m$  on  $\tau_j$ . Then by the definitions of  $P_h^-, P_h^+$ ,

$$\begin{aligned} (v - P_h^- v)(x) &= \bar{v}_{j,k} L_{j,k} + \sum_{m=k+1}^{\infty} v_{j,m} L_{j,m}(x), \\ (v - P_h^+ v)(x) &= \tilde{v}_{j,k} L_{j,k} + \sum_{m=k+1}^{\infty} v_{j,m} L_{j,m}(x), \end{aligned}$$

where

$$\bar{v}_{j,k} = -v(x_{j+\frac{1}{2}}^-) + \frac{1}{h_j} \int_{\tau_j} v(x) \sum_{m=0}^k (2m+1) L_{j,m}(x) dx, \quad (3.2)$$

$$\tilde{v}_{j,k} = (-1)^{k+1} v(x_{j-\frac{1}{2}}^+) + \frac{1}{h_j} \int_{\tau_j} v(x) \sum_{m=0}^k (-1)^{k+m} (2m+1) L_{j,m}(x) dx. \quad (3.3)$$

Apparently, the orthogonal properties of Legendre polynomials give

$$(v - P_h^- v, w)_j = \bar{v}_{j,k} (L_{j,k}, w)_j, \quad (v - P_h^+ v, w)_j = \tilde{v}_{j,k} (L_{j,k}, w)_j, \quad \forall w \in V_h. \quad (3.4)$$

To end this subsection, we would like to introduce a class of special functions, which play an important role in our superconvergence analysis. In each element  $\tau_j, j \in \mathbb{Z}_N$ , we define

$$F_{1,1} = P_h^+ D_s^{-1} L_{j,k}, \quad F_{1,i+1} = P_h^+ D_s^{-1} F_{2,i}, \quad 1 \leq i \leq k-1, \quad (3.5)$$

$$F_{2,1} = P_h^- D_s^{-1} L_{j,k}, \quad F_{2,i+1} = P_h^- D_s^{-1} F_{1,i}, \quad 1 \leq i \leq k-1. \quad (3.6)$$

Here the integral operator  $D_s^{-1}$  is defined by

$$D_s^{-1} v(x) = \frac{1}{h_j} \int_{x_{j-\frac{1}{2}}}^x v(x') dx' = \int_{-1}^s \hat{v}(s') ds', \quad x \in \tau_j, \quad j \in \mathbb{Z}_N$$

with

$$s = (x - x_j) / \bar{h}_j \in [-1, 1], \quad \hat{v}(s) = v(x).$$

We have the following properties of  $F_{r,i}, (r, i) \in \mathbb{Z}_2 \times \mathbb{Z}_k$  (see [9], Lemma 3.1)

$$F_{1,i}(x_{j-\frac{1}{2}}^+) = 0, \quad \|F_{1,i}\|_{0,\infty,\tau_j} \lesssim 1, \quad (F_{1,i}, v)_j = 0, \quad \forall v \in \mathbb{P}^{k-i-1}, \quad (3.7)$$

$$F_{2,i}(x_{j+\frac{1}{2}}^-) = 0, \quad \|F_{2,i}\|_{0,\infty,\tau_j} \lesssim 1, \quad (F_{2,i}, v)_j = 0, \quad \forall v \in \mathbb{P}^{k-i-1}. \quad (3.8)$$

Here and below, the notation  $A \lesssim B$  means that  $A$  can be bounded by  $B$  multiplied by a constant independent of the mesh size  $h$ . By the orthogonal properties of Legendre polynomials, it is easy to show that

$$D_s^{-1} L_{j,m}(x_{j+\frac{1}{2}}^-) = D_s^{-1} L_{j,m}(x_{j-\frac{1}{2}}^+) = 0, \quad \forall m \geq 1, \quad (3.9)$$

which yields (together with the third formulas of (3.7)-(3.8)),

$$D_s^{-1} F_{r,i}(x_{j+\frac{1}{2}}^-) = D_s^{-1} F_{r,i}(x_{j-\frac{1}{2}}^+) = 0, \quad (r, i) \in \mathbb{Z}_2 \times \mathbb{Z}_{k-1}. \quad (3.10)$$

### 3.2 Construction of special interpolation functions

To study superconvergence properties, our basis idea is to construct special interpolation functions  $(u_I, q_I)$  such that  $(u_I, q_I)$  are superclose to  $(u_h, q_h)$ . By the supercloseness between  $(u_I, q_I)$  and  $(u_h, q_h)$ , we obtain superconvergence properties of the LDG solution at some special points. our analysis is along this line.

We denote

$$e_v = v - v_h, \quad \xi_v = v_h - v_I, \quad \eta_v = v - v_I, \quad v = u, q.$$

Note that if we choose test functions  $(v, p) = ((\xi_u)_t, \xi_q)$  in the formula of  $\mathcal{A}(\xi_u, \xi_q; v, p)$  and use the periodic boundary condition, we derive

$$\begin{aligned} \frac{1}{2} \frac{d}{dt} \left( \|(\xi_u)_t\|_0^2 + \|\xi_q\|_0^2 - \alpha \|\xi_u\|_0^2 \right) &= \mathcal{A}(\xi_u, \xi_q; (\xi_u)_t, \xi_q) \\ &= \mathcal{A}(\eta_u, \eta_q; (\xi_u)_t, \xi_q), \end{aligned} \tag{3.11}$$

where in the last step, we have used the orthogonal properties  $\mathcal{A}(e_u, e_q; v, p) = 0, v, p \in V_h$ . Therefore, to achieve the supercloseness goal, the functions  $(u_I, q_I)$  should be carefully designed such that  $\mathcal{A}(\eta_u, \eta_q; v, p), \forall v, p \in V_h$ , is of high order.

In the rest of this subsection, we will first construct the special functions  $(u_I, q_I)$ , and then analyze their properties. We first consider the fluxes choice (2.4), in which case,

$$(u - P_h^- u, v)_j = \bar{u}_{j,k}(t)(L_{j,k}, v)_j, \quad (q - P_h^+ q, v)_j = \tilde{q}_{j,k}(t)(L_{j,k}, v)_j, \quad \forall v \in V_h, \tag{3.12}$$

where  $\bar{u}_{j,k}$  and  $\tilde{q}_{j,k}$  are given by (3.2)-(3.3). Let

$$G_1 = \tilde{q}_{j,k}, \quad Q_1 = (\partial_t^2 - \alpha)\bar{u}_{j,k}, \quad G_{i+1} = Q_i, \quad Q_{i+1} = (\partial_t^2 - \alpha)G_i, \quad i \geq 1. \tag{3.13}$$

Then for any given  $l, 1 \leq l \leq k$ , we define correction functions in each element  $\tau_j, j \in \mathbb{Z}_N$  as

$$w_u^l = \sum_{i=1}^l w_{u,i}, \quad w_q^l = \sum_{i=1}^l w_{q,i} \tag{3.14}$$

where

$$w_{u,i} = (\bar{h}_j)^i G_i F_{2,i}, \quad w_{q,i} = (\bar{h}_j)^i Q_i F_{1,i}, \quad 1 \leq i \leq l \tag{3.15}$$

with  $F_{r,i}$  defined by (3.5)-(3.6). Apparently, we have from (3.7)-(3.8)

$$\partial_t^r w_{u,i}(x_{j+\frac{1}{2}}^-) = 0, \quad w_{q,i}(x_{j-\frac{1}{2}}^+) = 0, \quad r = 0, 1, \quad 1 \leq i \leq l,$$

which yields

$$\partial_t^r w_u^l(x_{j+\frac{1}{2}}^-) = 0, \quad w_q^l(x_{j-\frac{1}{2}}^+) = 0, \quad r = 0, 1. \tag{3.16}$$

With the correction functions  $w_u^l, w_q^l, 1 \leq l \leq k$ , we define the special interpolation functions

$$(u_I, q_I) = (u_I^l, q_I^l) = (P_h^- u - w_u^l, P_h^+ q - w_q^l). \tag{3.17}$$

The procedure of constructing interpolation functions  $(u_I, q_I)$  for fluxes (2.5) is similar to that for fluxes (2.4). For fluxes (2.5), we define

$$(u_I, q_I) = (u_I^l, q_I^l) = (P_h^+ u - w_u^l, P_h^- q - w_q^l), \quad (3.18)$$

where

$$w_u^l = \sum_{i=1}^l w_{u,i} = \sum_{i=1}^l (\bar{h}_j)^i G_i F_{1,i}, \quad w_q^l = \sum_{i=1}^l w_{q,i} = \sum_{i=1}^l (\bar{h}_j)^i Q_i F_{2,i} \quad (3.19)$$

with

$$G_1 = \bar{q}_{j,k}, \quad Q_1 = (\partial_t^2 - \alpha) \bar{u}_{j,k}, \quad G_{i+1} = Q_i, \quad Q_{i+1} = (\partial_t^2 - \alpha) G_i, \quad i \geq 1. \quad (3.20)$$

**Lemma 3.1.** *Let the interpolation functions  $(u_I, q_I)$  be defined by (3.17) and (3.18) for fluxes (2.4) and (2.5), respectively. Then for both fluxes (2.4)-(2.5),*

$$\partial_t^r \hat{u}_I(x_{j-\frac{1}{2}}) = u(x_{j-\frac{1}{2}}), \quad \hat{q}_I(x_{j-\frac{1}{2}}) = q(x_{j-\frac{1}{2}}), \quad r = 0, 1. \quad (3.21)$$

Moreover, there holds for any  $v \in V_h$

$$((\partial_{tt} - \alpha) \eta_{u,v}) + (\eta_{q,v_x}) = ((\partial_{tt} - \alpha) w_{u,l}, v), \quad (\eta_{q,v}) + (\eta_{u,v_x}) = (w_{q,l}, v). \quad (3.22)$$

*Proof.* We only consider the flux choice (2.4) since the same argument can be applied to flux (2.5). By (3.16)-(3.17), and the properties of  $P_h^-, P_h^+$ , we get (3.21) directly for the flux (2.4).

We next show (3.22). By (3.12)-(3.13), (3.9), and the integration by parts, there hold for all  $v, p \in V_h$

$$((\partial_t^2 - \alpha)(u - P_h^- u), v)_j = -\bar{h}_j Q_1 (D_s^{-1} L_{j,k}, v_x)_j = -(w_{q,1}, v_x)_j, \quad (3.23)$$

$$((q - P_h^+ q), p)_j = -\bar{h}_j G_1 (D_s^{-1} L_{j,k}, p_x)_j = -\bar{h}_j G_1 (F_{2,1}, p_x)_j = -(w_{u,1}, p_x)_j. \quad (3.24)$$

On the other hand, by the integration by parts, (3.10), (3.13), and (3.5)-(3.6), we have for all  $1 \leq i \leq l-1$ ,

$$\begin{aligned} ((\partial_t^2 - \alpha) w_{u,i}, v)_j &= (\bar{h}_j)^i (\partial_t^2 - \alpha) G_i (F_{2,i}, v)_j = -(\bar{h}_j)^{i+1} Q_{i+1} (D_s^{-1} F_{2,i}, v_x)_j \\ &= -(\bar{h}_j)^{i+1} Q_{i+1} (F_{1,i+1}, v_x)_j = -(w_{q,i+1}, v_x)_j, \\ (w_{q,i}, v)_j &= (\bar{h}_j)^i \partial_t Q_i (F_{1,i}, v)_j = -(\bar{h}_j)^{i+1} G_{i+1} (D_s^{-1} F_{1,i}, v_x)_j \\ &= -(\bar{h}_j)^{i+1} G_{i+1} (F_{2,i+1}, v_x)_j = -(w_{u,i+1}, v_x)_j. \end{aligned}$$

Consequently,

$$\begin{aligned} ((\partial_t^2 - \alpha) w_u^l, v) + (w_q^l, v_x) &= ((\partial_t^2 - \alpha) w_{u,l}, v) + (w_{q,1}, v_x), \\ (w_q^l, p) + (w_u^l, p_x) &= (w_{q,l}, p) + (w_{u,1}, p_x), \end{aligned}$$

which yields, together with (3.23)-(3.24), the desired result (3.22). This finishes our proof.  $\square$

**Lemma 3.2.** For any given  $l$ , where  $1 \leq l \leq k$ , let  $u \in W^{k+l+2,\infty}(\Omega)$ , and  $w_v^l (v = u, q)$  be defined by (3.14) or (3.19). Then

$$\|w_u^l\|_{0,\infty} + \|w_q^l\|_{0,\infty} \lesssim h^{k+2} \|u\|_{k+l+2,\infty}. \tag{3.25}$$

Moreover, if  $u \in W^{k+l+3,\infty}(\Omega), \partial_t u \in W^{k+l+2,\infty}(\Omega)$ , then for both fluxes (2.4) and (2.5),

$$\mathcal{A}(\eta_u, \eta_q; v, p) \lesssim h^{k+l+1} \left( \|u\|_{k+3+l,\infty} + \|\partial_t u\|_{k+2+l,\infty} \right) \left( \|v\|_{0,1} + \|p\|_{0,1} \right). \tag{3.26}$$

*Proof.* If  $w_v^l, v = u, q$  is defined by (3.14), then a direct calculation from (3.13) yields

$$\begin{aligned} G_i &= (\partial_t^2 - \alpha)^r \bar{u}_{j,k}, & Q_i &= (\partial_t^2 - \alpha)^r \tilde{q}_{j,k}, & \text{if } i = 2r, \\ G_i &= (\partial_t^2 - \alpha)^r \tilde{q}_{j,k}, & Q_i &= (\partial_t^2 - \alpha)^{r+1} \bar{u}_{j,k}, & \text{if } i = 2r + 1. \end{aligned}$$

Since  $\bar{u}_{j,k} = \tilde{q}_{j,k} = 0$  when  $u, q \in \mathbb{P}^k(\tau_j)$ , we have, from the Bramble-Hilbert lemma

$$|\bar{u}_{j,k}| \lesssim h^{k+1} \|\partial_x^{k+1} u\|_{0,\infty,\tau_j}, \quad |\tilde{q}_{j,k}| \lesssim h^{k+1} \|\partial_x^{k+1} q\|_{0,\infty,\tau_j},$$

Consequently, by using the fact that  $\partial_t^2 u = \partial_x^2 u + \alpha u$  and  $q = u_x$ , we have for any positive integer  $r$

$$|\partial_t^r G_i|_{0,\infty,\tau_j} \lesssim h^{k+1} \|\partial_t^r u\|_{k+1+i,\infty,\tau_j}, \quad |\partial_t^r Q_i|_{0,\infty,\tau_j} \lesssim h^{k+1} \|\partial_t^r u\|_{k+2+i,\infty,\tau_j},$$

which yields

$$\|\partial_t^r w_{u,i}\|_{0,\infty,\tau_j} \lesssim h^{k+1+i} \|\partial_t^r u\|_{k+1+i,\infty,\tau_j}, \quad \|\partial_t^r w_{q,i}\|_{0,\infty,\tau_j} \lesssim h^{k+1+i} \|\partial_t^r u\|_{k+2+i,\infty,\tau_j}. \tag{3.27}$$

Hence, the desired result (3.25) follows. If  $w_v^l, v = u, q$  is defined by (3.19), (3.25) still holds true by using the same argument.

By (3.21), the orthogonalities of  $P_h^-, P_h^+$ , and (3.22), we get

$$\begin{aligned} \mathcal{A}(\eta_u, \eta_q; v, p) &= ((\partial_t^2 - \alpha)\eta_u, v) + (\eta_q, v_x) + (\partial_t \eta_q, p) + (\partial_t \eta_u, p_x) \\ &= ((\partial_t^2 - \alpha)w_{u,l}, v) + (\partial_t w_{q,l}, p), \quad \forall v, p \in V_h. \end{aligned}$$

Then (3.26) follows from (3.27). □

### 3.3 Superconvergence results

We first analyze the supercloseness between the LDG solution  $(u_h, q_h)$  and the specially designed interpolation functions  $(u_I, q_I)$  defined by (3.17) or (3.18). Without loss of generality, we only consider three special cases. That is,

$$f(u) = \alpha u, \quad \alpha = 0, \pm 1.$$

The same arguments can be applied to a general case in which  $\alpha$  is an arbitrary constant.

**Theorem 3.1.** Let  $u \in W^{k+l+3,\infty}(\Omega)$ ,  $\partial_t u \in W^{k+l+2,\infty}(\Omega)$ , and  $(u_I^l, q_I^l)$  be defined by (3.17) or (3.18). Let  $(u_h, q_h)$  be the solution of (3.1) with initial values  $u_h(x,0) = u_I^l(x,0)$ ,  $\partial_t u_h(x,0) = \partial_t u_I^l(x,0)$ . Then for fluxes (2.4) and (2.5),

$$\left( \| (u_I^l - u_h)_t \|_0 + \| u_I^l - u_h \|_0 + \| q_I^l - q_h \|_0 \right) (t) \lesssim h^{k+l+1} c(u). \quad (3.28)$$

Here  $c(u) = \|u\|_{k+l+3,\infty} + \|\partial_t u\|_{k+l+2,\infty}$ .

*Proof.* By (3.11) and (3.26), we have

$$\frac{1}{2} \frac{d}{dt} \left( \|(\xi_u)_t\|_0^2 + \|\xi_q\|_0^2 - \alpha \|\xi_u\|_0^2 \right) \lesssim h^{k+l+1} c(u) \left( \|(\xi_u)_t\|_0 + \|\xi_q\|_0 \right). \quad (3.29)$$

When  $\alpha = -1$ , by Gronwall's inequality and the special choice of initial values,

$$\left( \|(\xi_u)_t\|_0 + \|\xi_q\|_0 + \|\xi_u\|_0 \right) (t) \lesssim h^{k+l+1} c(u) + \|\xi_q\|_0(0).$$

At the initial time  $t=0$ , thanks to the special choice of the initial solution and (3.21),

$$(\eta_q, p)(0) - (\xi_q, p)(0) = (e_q, p)(0) = -\mathcal{D}(e_u, p; \hat{e}_u)|_{t=0} = -(\eta_u, p_x)(0).$$

By choosing  $p = \xi_q$  and using (3.22) and (3.27), we obtain

$$\|\xi_q\|_0(0) \lesssim \|w_{q,l}\|_{0,\infty}(0) \lesssim h^{k+l+1} \|u\|_{k+l+2,\infty}.$$

Then (3.28) follows.

Similarly, when  $\alpha = 0$ , we first obtain, from (3.29) and the estimate for  $\|\xi_q\|_0(0)$ ,

$$\left( \| (u_I^l - u_h)_t \|_0 + \| q_I^l - q_h \|_0 \right) (t) \lesssim h^{k+l+1} c(u).$$

To estimate  $\|\xi_u\|_0$ , we integrate both sides of (3.1) from  $t$  to  $\tau$  and use the orthogonality to obtain

$$(\partial_{tt} e_u, v) + \mathcal{D}(e_q, v, \hat{e}_q) + \int_t^\tau (e_q, p) + \int_t^\tau \mathcal{D}(e_u, p, \hat{e}_u) = 0. \quad (3.30)$$

On the other hand, noticing that (3.22) holds true for all  $v \in V_h$ , then

$$\int_t^\tau ((\eta_q, v) + (\eta_u, v_x)) = \int_t^\tau (w_{q,l}, v) = (E_q^l, v),$$

where  $E_q^l = \int_t^\tau w_{q,l}(t) dt$ . Let

$$E_u = \int_t^\tau \xi_u(t) dt, \quad E_q = \int_t^\tau \xi_q(t) dt.$$

Choosing  $(v, p) = (E_u, \xi_q)$  in (3.30) and using (3.22) gives

$$\begin{aligned} \frac{1}{2} \frac{d}{dt} (\|\xi_u\|_0^2 - \|E_q\|_0^2) &= -\frac{d}{dt} (\partial_t \xi_u, E_u) + (\partial_{tt} \eta_u, E_u) + (\eta_q, (E_u)_x) + (E_q^l, \xi_q) \\ &= -\frac{d}{dt} (\partial_t \xi_u, E_u) + (\partial_{tt} w_{u,l}, E_u) + (E_q^l, \xi_q) \\ &= -\frac{d}{dt} (\partial_t (\xi_u - w_{u,l}), E_u) + (\partial_t w_{u,l}, \xi_u) + (E_q^l, \xi_q). \end{aligned}$$

Integrating the inequality from 0 to  $\tau$  and using the fact that  $E_v(\tau) = 0, v = u, q$ , we get

$$\begin{aligned} \frac{1}{2} \|\xi_u(\tau)\|_0^2 - \frac{1}{2} \|\xi_u(0)\|_0^2 &\leq |(\partial_t (\xi_u - w_{u,l}), E_u)(0)| + CT \max_{t \in [0, T]} \left( \|E_q^l\|_0 \|\xi_q\|_0 + \|(w_{u,l})_t\|_0 \|\xi_u\|_0 \right) \\ &\leq |(\partial_t \xi_u, E_u)(0)| + C(T+1)^2 h^{2(k+l+1)} c(u)^2 + \frac{1}{4} \max_{t \in [0, T]} \|\xi_u\|_0^2. \end{aligned}$$

Here in the last step, we have used (3.27). Consequently, if the initial solution satisfies  $\xi_u(0) = \partial_t \xi_u(0) = 0$ , then

$$\max_{t \in [0, T]} \|\xi_u\|_0 \lesssim h^{k+l+1} c(u).$$

Then (3.28) follows.

Now we consider  $\alpha = 1$ . By (3.29), Gronwall's inequality and the special choice of initial values,

$$\|(\xi_u)_t(\tau)\|_0^2 + \|\xi_q(\tau)\|_0^2 \leq Ch^{2(k+l+1)} c(u)^2 + 2\|\xi_u(\tau)\|_0^2, \quad \forall \tau \geq 0. \tag{3.31}$$

Following the same argument as in the case  $\alpha = 0$ , we obtain

$$\frac{1}{2} \frac{d}{dt} (\|\xi_u\|_0^2 + \|E_u\|_0^2 - \|E_q\|_0^2) = -\frac{d}{dt} (\partial_t \xi_u, E_u) + ((\partial_{tt} - 1)w_{u,l}, E_u) + (E_q^l, \xi_q).$$

For any fixed  $t_0 \geq 0$ , integrating the above equation from  $t_0$  to  $\tau$ , and using Cauchy-Schwartz inequality, we get

$$\begin{aligned} \frac{1}{2} \|\xi_u(\tau)\|_0^2 - \frac{1}{2} \|\xi_u(t_0)\|_0^2 &\leq \|E_u(t_0)\|_0^2 + \frac{1}{2} \|(\xi_u)_t(t_0)\|_0^2 + \frac{1}{16} \max_{t \in [t_0, \tau]} (\|\xi_u\|_0^2 + \|\xi_q\|_0^2) \\ &\quad + C(\tau - t_0)^2 h^{2(k+l+1)} c(u)^2 \\ &\leq \|\xi_u(t_0)\|_0^2 + \left( (\tau - t_0)^2 + \frac{3}{16} \right) \max_{t \in [t_0, \tau]} \|\xi_u\|_0^2 + C(\tau - t_0)^2 h^{2(k+l+1)} c(u)^2, \end{aligned}$$

where in the last step, we have used (3.31) and the fact

$$\|E_u(t_0)\|_0^2 \leq (\tau - t_0)^2 \max_{t \in [t_0, \tau]} \|\xi_u(t)\|_0^2.$$

Therefore, for any  $\tau$  satisfying  $(\tau - t_0) \leq \frac{1}{4}$ , we get

$$\|\xi_u(\tau)\|_0^2 \lesssim \|\xi_u(t_0)\|_0^2 + h^{2(k+l+1)}c(u)^2.$$

Then for all  $t \in [0, T]$ ,

$$\|\xi_u(t)\|_0^2 \lesssim \|\xi_u(0)\|_0^2 + h^{2(k+l+1)}c(u)^2 \lesssim h^{2(k+l+1)}c(u)^2.$$

Plugging the above estimate into (3.31) yields

$$\|(\xi_u)_t\|_0 + \|\xi_q\|_0 \lesssim h^{k+l+1}c(u).$$

Then (3.28) follows. The proof is complete. □

As a direct consequence of (3.28) and (3.25), we have the following superconvergence results for the Gauss-Radau projection of the exact solution.

**Corollary 3.1.** *Let  $u \in W^{k+4,\infty}(\Omega)$ ,  $\partial_t u \in W^{k+3,\infty}(\Omega)$ , and  $(u_h, q_h)$  be the solution of (3.1). Suppose the initial values are chosen as  $u_h(x, 0) = u_1^l(x, 0)$ ,  $\partial_t u_h(x, 0) = \partial_t u_1^l(x, 0)$  with  $l = 1$ . Then for fluxes (2.4) and (2.5),*

$$\|u_h - P_h u\|_0 + \|q_h - P_h q\|_0 \lesssim h^{k+2} (\|u\|_{k+4,\infty} + \|\partial_t u\|_{k+3,\infty}), \tag{3.32}$$

where  $(P_h u, P_h q) = (P_h^- u, P_h^+ q)$  for fluxes (2.4) and  $(P_h u, P_h q) = (P_h^+ u, P_h^- q)$  for fluxes (2.5).

We first use the supercloseness result (3.28) to study the superconvergence for cell averages.

**Theorem 3.2.** *Let  $u \in W^{2k+3,\infty}(\Omega)$ ,  $\partial_t u \in W^{2k+2,\infty}(\Omega)$ , and  $(u_h, q_h)$  be the solution of (3.1). If the initial values are chosen as  $u_h(x, 0) = u_1^l(x, 0)$ ,  $\partial_t u_h(x, 0) = \partial_t u_1^l(x, 0)$  with  $l = k$ , then for fluxes (2.4) and (2.5),*

$$\|e_u\|_c + \|e_q\|_c \lesssim h^{2k+1} (\|u\|_{2k+3,\infty} + \|\partial_t u\|_{2k+2,\infty}), \tag{3.33}$$

where  $\|e_v\|_c, v = u, q$  denotes the cell average of function  $v$ , i.e.,

$$\|e_v\|_c = \left( \frac{1}{N} \sum_{j=1}^N \left( \frac{1}{h_j} \int_{\tau_j} e_v \right)^2 \right)^{\frac{1}{2}}.$$

*Proof.* Let  $v_I = v_I^k, v = u, q$ . It is straightforward to deduce from (3.7)-(3.8) that

$$w_{v,i} \perp \mathbb{P}^0, \quad 1 \leq i \leq k-1,$$

which yields, together with the properties of  $P_h^-, P_h^+$ ,

$$\int_{\tau_j} e_v = \int_{\tau_j} (\eta_v - \xi_v) = \int_{\tau_j} w_{v,k} - \int_{\tau_j} \xi_v.$$

Consequently, by (3.27) and (3.28),

$$\|e_v\|_c \lesssim \|\xi_v\|_0 + \|w_{v,k}\|_{0,\infty} \lesssim h^{2k+1} (\|u\|_{2k+3,\infty} + \|\partial_t u\|_{2k+2,\infty}).$$

This finishes our proof. □

Next we analyze the superconvergence properties at nodal points.

**Theorem 3.3.** *Suppose all the conditions of Theorem 3.2 hold. Then for both fluxes (2.4) and fluxes (2.5),*

$$\|e_u\|_* + \|e_q\|_* \lesssim h^{2k+1} (\|u\|_{2k+3,\infty} + \|\partial_t u\|_{2k+2,\infty}), \tag{3.34}$$

where

$$\|e_v\|_* = \left( \frac{1}{N} \sum_{j=1}^N (v - \hat{v}_h)^2(x_{j-\frac{1}{2}}, t) \right)^{\frac{1}{2}}, \quad v = u, q.$$

*Proof.* For any  $v \in V_h$ , the inverse inequality gives

$$\frac{1}{N} \sum_{j=1}^N \|v\|_{0,\infty,\tau_j}^2 \lesssim \frac{1}{N} \sum_{j=1}^N h_j^{-1} \|v\|_{0,\tau_j}^2 \lesssim \|v\|_0^2.$$

By choosing  $v = u_I - u_h, q_I - q_h$ , where  $(u_I, q_I)$  is defined by (3.17) or (3.18) with  $l = k$ , we immediately have

$$\|u_I - u_h\|_* + \|q_I - q_h\|_* \lesssim \|u_I - u_h\|_0 + \|q_I - q_h\|_0.$$

Then the desired result (3.34) follows from (3.28) and (3.21). □

**Remark 3.1.** Following the same line as in [10], we can prove the  $(2k+1)$ -th superconvergence rate for the pointwise error of numerical fluxes at nodes, that is,

$$\max_{j \in \mathbb{Z}_N} |(v - \hat{v}_h)(x_{j+\frac{1}{2}}, t)| \lesssim h^{2k+1}, \quad v = u, q.$$

However, the proof is more sophisticated and the regularity requirement for  $u$  is more stronger.

Let  $R_{j,m}^l, R_{j,m}^r, m \in \mathbb{Z}_k$  denote the  $k$  interior left and right Radau points in the interval  $\tau_j, j \in \mathbb{Z}_N$ , respectively. That is,  $R_{j,m}^l, m \in \mathbb{Z}_k$  are zeros of  $L_{j,k+1} + L_{j,k}$  except the point  $x = x_{j-\frac{1}{2}}$ , and  $R_{j,m}^r, m \in \mathbb{Z}_k$  are zeros of  $L_{j,k+1} - L_{j,k}$  except the point  $x = x_{j+\frac{1}{2}}$ . We have the following superconvergence results at these interior Radau points.

**Theorem 3.4.** *Let  $u \in W^{k+5,\infty}(\Omega)$ ,  $\partial_t u \in W^{k+4,\infty}(\Omega)$ , and  $(u_h, q_h)$  be the solution of (3.1). If the initial values are chosen as  $u_h(x, 0) = u_I^l(x, 0)$ ,  $\partial_t u_h(x, 0) = \partial_t u_I^l(x, 0)$  with  $l = 2$ , then for fluxes (2.4), there holds*

$$e_{u,r} + e_{q,l} \lesssim h^{k+2} c(u), \quad e_{u_x,l} + e_{q_x,r} \lesssim h^{k+1} c(u), \tag{3.35}$$

and for fluxes (2.5)

$$e_{u,l} + e_{q,r} \lesssim h^{k+2} c(u), \quad e_{u_x,r} + e_{q_x,l} \lesssim h^{k+1} c(u). \tag{3.36}$$

Here  $c(u) = \|u\|_{k+5,\infty} + \|\partial_t u\|_{k+4,\infty}$ , and for  $v = u, q$ ,

$$e_{v,r} = \max_{j,m} \left| (v - v_h)(R_{j,m}^r, t) \right|, \quad e_{v,l} = \max_{j,m} \left| (v - v_h)(R_{j,m}^l, t) \right|,$$

$$e_{vx,l} = \max_{j,m} \left| \partial_x (v - v_h)(R_{j,m}^l, t) \right|, \quad e_{vx,r} = \max_{j,m} \left| \partial_x (v - v_h)(R_{j,m}^r, t) \right|.$$

*Proof.* We only consider the fluxes (2.4) since the same argument can be applied to fluxes (2.5). For all  $v \in W^{k+2,\infty}(\Omega)$ , it is shown in [8, 9] that

$$\left| (v - P_h^- v)(R_{j,m}^r) \right| + \left| (v - P_h^+ v)(R_{j,m}^l) \right| \lesssim h^{k+2} \|v\|_{k+2,\infty}, \quad (3.37)$$

$$\left| \partial_x (v - P_h^- v)(R_{j,m}^l) \right| + \left| \partial_x (v - P_h^+ v)(R_{j,m}^r) \right| \lesssim h^{k+1} \|v\|_{k+2,\infty}. \quad (3.38)$$

Meanwhile, we choose  $l=2$  in (3.28) and use the inverse inequality to obtain

$$\|u_I - u_h\|_{0,\infty} + \|q_I - q_h\|_{0,\infty} \lesssim h^{-\frac{1}{2}} (\|u_I - u_h\|_0 + \|q_I - q_h\|_0) \lesssim h^{k+\frac{5}{2}} c(u).$$

Here  $u_I = u_I^l, q_I = q_I^l$  with  $l=2$ . Recalling the definition of  $(u_I, q_I)$  in (3.17), together with (3.25), we immediately have

$$\|u_h - P_h^- u\|_{0,\infty} + \|q_h - P_h^+ q\|_{0,\infty} \lesssim h^{k+2} c(u). \quad (3.39)$$

Then the first inequality of (3.35) follows by using (3.37), (3.39), and the triangular inequality. Similarly, we have, from the inverse inequality,

$$\|u_h - P_h^- u\|_{1,\infty} + \|q_h - P_h^+ q\|_{1,\infty} \lesssim h^{-1} (\|u_h - P_h^- u\|_{0,\infty} + \|q_h - P_h^+ q\|_{0,\infty}) \lesssim h^{k+1} c(u).$$

This completes the proof.  $\square$

In light of (3.38), the second inequality of (3.35) follows.

**Remark 3.2.** In Corollary 3.1 and Theorems 3.2-3.4, we choose different initial discretizations to achieve our superconvergence goals. However, all the superconvergence results in Corollary 3.1 and Theorems 3.3-3.4 are valid if we choose a unified initial values  $u_h(x,0) = u_I^k(x,0), \partial_t u_h(x,0) = \partial_t u_I^k(x,0)$ . The proof is the same as that in [8], which is due to the fact that the initial errors of the LDG solution are small enough to be compatible with the superconvergence error estimate.

## 4 Energy conservation

This section is devoted to developing energy conserving numerical methods for the non-linear wave equations.

### 4.1 A semi-discrete energy conserving algorithm

The semi-discrete LDG method conserves the energy in the following sense.

**Theorem 4.1.** *Let  $F(u) = \int f(u)du$ . Then the energy*

$$E_h(t) = \frac{1}{2} \int_{\Omega} \left( (u_h)_t^2 + q_h^2 - 2F(u_h) \right) dx,$$

*which is derived by the semi-discrete LDG method, is conserved for all time.*

*Proof.* For the sake of brevity, we omit the detailed proof here since it follows along the same analysis in proving the first equality of (3.11). □

### 4.2 A fully discrete energy conserving scheme

We divide the time interval  $[0, T]$  uniformly with the time step size  $\Delta t = T/M$ , where  $M$  is a given positive integer. Then, our fully discrete numerical scheme for problem (1.1) is as follows: for  $m = 1, \dots, M-1$ ,

$$\begin{aligned} & \int_{\tau_j} \frac{u_h^{m+3} - u_h^{m+2} - u_h^{m+1} + u_h^m}{2\Delta t^2} v dx + \int_{\tau_j} \frac{q_h^{m+2} + q_h^{m+1}}{2} v_x dx - \left( \frac{\hat{q}_h^{m+2} + \hat{q}_h^{m+1}}{2} v^- \right)_{j+\frac{1}{2}} \\ & + \left( \frac{\hat{q}_h^{m+2} + \hat{q}_h^{m+1}}{2} v^+ \right)_{j-\frac{1}{2}} - \int_{\tau_j} \frac{F(u_h^{m+2}) - F(u_h^{m+1})}{u_h^{m+2} - u_h^{m+1}} v dx = 0, \end{aligned} \tag{4.1}$$

$$\int_{\tau_j} q_h^m p dx + \int_{\tau_j} u_h^m p_x dx - (\hat{u}_h^m p^-)_{j+\frac{1}{2}} + (\hat{u}_h^m p^+)_{j-\frac{1}{2}} = 0, \tag{4.2}$$

where  $u_h^m$  and  $q_h^m$  are numerical approximations to  $u(\cdot, t_m)$  and  $q(\cdot, t_m)$ , respectively, and  $v, p \in V_h$ .

The above explicit scheme has second-order accuracy in time according to the Taylor expansion at the time  $(m + \frac{1}{2})\Delta t$ . In addition, we have the following energy preserving property.

**Theorem 4.2.** *The numerical solution that derived by the fully discrete numerical method (4.1)-(4.2) conserves the following discrete energy*

$$E_h^{m+1} = \int_{\Omega} \left( \frac{(u_h^{m+2} - u_h^{m+1})(u_h^{m+1} - u_h^m)}{2\Delta t^2} + \frac{1}{2}(q_h^{m+1})^2 - F(u_h^{m+1}) \right) dx$$

*for all  $m$ .*

*Proof.* Taking the test function  $v = u_h^{m+2} - u_h^{m+1}$  in Eq. (4.1), we have

$$\begin{aligned} & \int_{\tau_j} \frac{u_h^{m+3} - u_h^{m+2} - u_h^{m+1} + u_h^m}{2\Delta t^2} (u_h^{m+2} - u_h^{m+1}) dx + \int_{\tau_j} \frac{q_h^{m+2} + q_h^{m+1}}{2} (u_h^{m+2} - u_h^{m+1})_x dx \\ & - \left( \frac{\hat{q}_h^{m+2} + \hat{q}_h^{m+1}}{2} (u_h^{m+2} - u_h^{m+1})^- \right)_{j+\frac{1}{2}} + \left( \frac{\hat{q}_h^{m+2} + \hat{q}_h^{m+1}}{2} (u_h^{m+2} - u_h^{m+1})^+ \right)_{j-\frac{1}{2}} \\ & - \int_{\tau_j} \left( F(u_h^{m+2}) - F(u_h^{m+1}) \right) dx = 0, \end{aligned} \tag{4.3}$$

Consider Eq. (4.2) at different time levels  $(m+2)\Delta t$  and  $(m+1)\Delta t$ , subtract the two and take the test function  $p = \frac{q_h^{m+2} + q_h^{m+1}}{2}$  gives

$$\begin{aligned} & \int_{\tau_j} (q_h^{m+2} - q_h^{m+1}) \frac{q_h^{m+2} + q_h^{m+1}}{2} dx + \int_{\tau_j} (u_h^{m+2} - u_h^{m+1}) \left( \frac{q_h^{m+2} + q_h^{m+1}}{2} \right)_x dx \\ & - \left( (\hat{u}_h^{m+2} - \hat{u}_h^{m+1}) \left( \frac{q_h^{m+2} + q_h^{m+1}}{2} \right)^- \right)_{j+\frac{1}{2}} + \left( (\hat{u}_h^{m+2} - \hat{u}_h^{m+1}) \left( \frac{q_h^{m+2} + q_h^{m+1}}{2} \right)^+ \right)_{j-\frac{1}{2}} = 0. \end{aligned} \tag{4.4}$$

Adding (4.3) and (4.4) and summing over for  $j$  from 1 to  $N$ , we obtain

$$\begin{aligned} & \int_{\tau_j} \frac{u_h^{m+3} - u_h^{m+2} - u_h^{m+1} + u_h^m}{2\Delta t^2} (u_h^{m+2} - u_h^{m+1}) dx + \int_{\tau_j} (q_h^{m+2} - q_h^{m+1}) \frac{q_h^{m+2} + q_h^{m+1}}{2} dx \\ & - \int_{\tau_j} \left( F(u_h^{m+2}) - F(u_h^{m+1}) \right) dx = 0, \end{aligned} \tag{4.5}$$

where we have used that fact that the other terms at the boundary cells vanish.

Eq. (4.5) can be rewritten as

$$\begin{aligned} & \int_{\Omega} \left( \frac{(u_h^{m+3} - u_h^{m+2})(u_h^{m+2} - u_h^{m+1})}{2\Delta t^2} + \frac{1}{2} (q_h^{m+2})^2 - F(u_h^{m+2}) \right) dx \\ & - \int_{\Omega} \left( \frac{(u_h^{m+2} - u_h^{m+1})(u_h^{m+1} - u_h^m)}{2\Delta t^2} + \frac{1}{2} (q_h^{m+1})^2 - F(u_h^{m+1}) \right) dx = 0 \end{aligned} \tag{4.6}$$

Therefore,

$$E_h^{m+2} = E_h^{m+1},$$

which completes the proof. □

**Remark 4.1.** Our fully discrete numerical scheme is explicit. Meanwhile, the conservation of the discrete energy is a numerical simulation of the energy conservation at the

continuous level. On the contrary, some classical difference methods, e.g.,

$$\int_{\tau_j} \frac{u_h^{m+2} - 2u_h^{m+1} + u_h^m}{\Delta t^2} v dx + \int_{\tau_j} q_h^{m+1} v_x dx - (\hat{q}_h^{m+1} v^-)_{j+\frac{1}{2}} + (\hat{q}_h^{m+1} v^+)_{j-\frac{1}{2}} - \int_{\tau_j} f(u_h^{m+1}) v_h dx = 0, \tag{4.7}$$

may not conserve the discrete energy for nonlinear problems. This will be illustrated by a sequence of numerical experiments. Another widely used finite difference method, i.e.,

$$\int_{\tau_j} \frac{u_h^{m+2} - 2u_h^{m+1} + u_h^m}{\Delta t^2} v dx + \int_{\tau_j} q_h^{m+1} v_x dx - (\hat{q}_h^{m+1} v^-)_{j+\frac{1}{2}} + (\hat{q}_h^{m+1} v^+)_{j-\frac{1}{2}} - \int_{\tau_j} \frac{F(u_h^{m+2}) - F(u_h^m)}{u_h^{m+2} - u_h^m} v_h dx = 0, \tag{4.8}$$

also conserves energy. However, the method is implicit. The computational cost is rather high.

**Remark 4.2.** Since the proposed numerical method (4.1) requires initial conditions for three time steps, we apply the following strategies. First, we rewrite (1.1) as

$$u_t = w, \quad w_t - q_x = f(u), \quad q - u_x = 0, \tag{4.9}$$

with initial conditions  $u(x,0) = u_0(x,0)$  and  $w(x,0) = u_t(x,0)$ . Then, we apply a high-order TVD Runge-Kutta method to compute the numerical solutions at the first three time steps.

**Remark 4.3.** In the case of homogeneous Dirichlet boundary condition  $u(a,t) = 0, u(b,t) = 0$ , we can still have the discrete conserved energy. The only difference is that the numerical fluxes at the boundaries should be defined by

$$(\hat{q}_h)_{\frac{1}{2}} = q_h(x_{\frac{1}{2}}^+), \quad (\hat{u}_h)_{\frac{1}{2}} = u(a,t) = 0, \\ (\hat{q}_h)_{N+\frac{1}{2}} = q_h(x_{N+\frac{1}{2}}^-), \quad (\hat{u}_h)_{N+\frac{1}{2}} = u(b,t) = 0.$$

The proof is similar to that in the periodic boundary condition.

## 5 Numerical experiments

In this section, we present several numerical experiments to illustrate our theoretical findings.

### 5.1 Superconvergence

We will test the superconvergence results in Section 3. If not otherwise stated, the initial discretizations are chosen as  $u_h(x,0) = u_I^k(x,0)$ ,  $\partial_t u_h(x,0) = \partial_t u_I^k(x,0)$ .

**Example 1.** We consider the following equation

$$u_{tt} + u = u_{xx}, \quad (x,t) \in (0,2\pi) \times (0,1)$$

with the periodic boundary condition  $u(0,t) = u(2\pi,t)$  and initial conditions

$$u(x,0) = \sin(x), \quad u_t(x,0) = \sqrt{2}\cos(x).$$

The exact solution is

$$u(x,t) = \sin(x + \sqrt{2}t).$$

We apply the scheme (3.1) with polynomial degree  $k=2,3,4$ . Numerical fluxes are chosen as (2.4). Piecewise uniform meshes are constructed by equally dividing each interval,  $[0, \frac{3\pi}{4}]$  and  $[\frac{3\pi}{4}, 2\pi]$ , into  $N/2$  subintervals with  $N = 2^m$ , where  $m = 3,4, \dots, 8$  for  $k = 2,3$ , and  $m = 3,4, \dots, 7$  for  $k = 4$ . To reduce the time discretization error, we use the ninth-order strong-stability preserving (SSP) Runge-Kutta method [20] with time step  $\Delta t = 0.001h_{\min}$ ,  $h_{\min} = \frac{3\pi}{2N}$ .

In Tables 1-3, we list numerical data for various errors defined in Theorems 3.2-3.4. We also plot in Figs. 1-3 the corresponding error curves with log-log scale. We observe a  $2k+1$  convergence rate for  $\|e_{v,n}\|_{*}, \|e_v\|_c, v = u, q$ , and a  $k+2$  rate for  $e_{u,r}, e_{q,l}$ , as predicted by Theorems 3.2-3.4. Moreover, we also observe a convergence rate of  $k+2$  for  $e_{ux,l}, e_{qx,r}$ ,

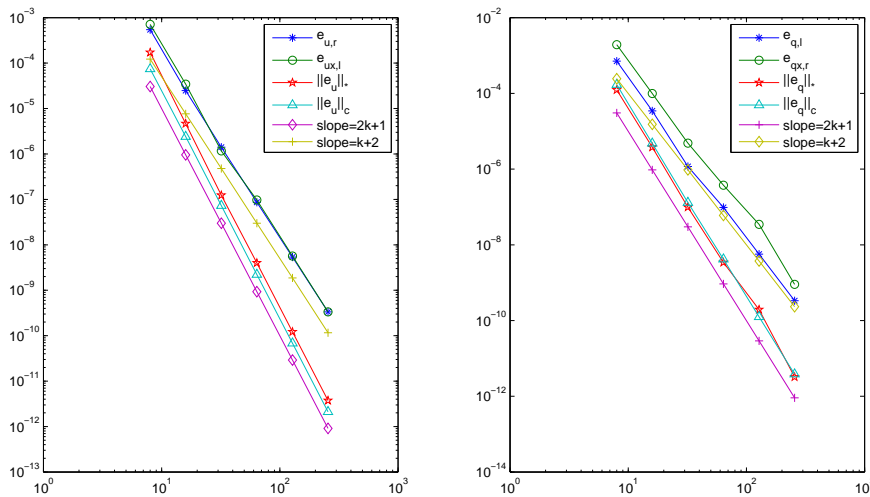


Figure 1: Error curves for  $k=2$ .

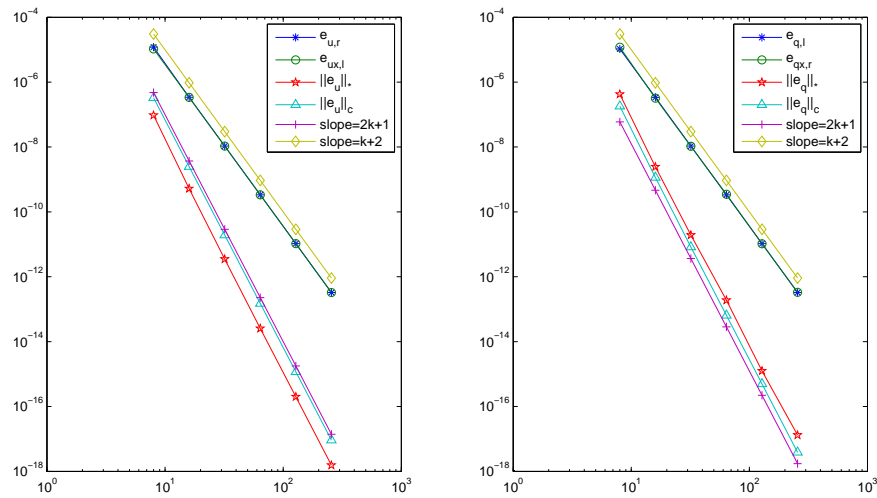


Figure 2: Error curves for  $k=3$ .

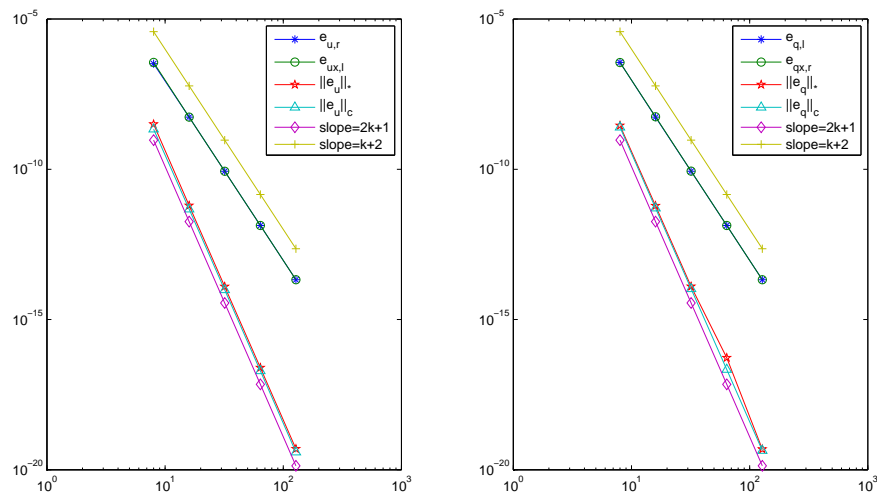


Figure 3: Error curves for  $k=4$ .

which implies that the derivative errors  $\partial_x(u - u_h)$  and  $\partial_x(q - q_h)$  are superconvergent at all interior left and right Radau points, respectively, with an order  $k+2$ . Note that the convergence rate  $k+2$  for the derivative approximation is one-order higher than the one given in (3.35).

To show the influence of the initial discretization on the convergence rate, we also discretize the initial solution with the  $L^2$ -projection, i.e.,  $\partial_t^i u_h(x, 0) = R_h \partial_t^i u(x, 0), i=0, 1$ . Here  $R_h u$  denotes the  $L^2$ -projection of  $u$ . The results and the corresponding convergence rates

Table 1: Various errors for  $k=2$ .

N	$e_{u,r}$	$e_{ux,l}$	$\ e_u\ _*$	$\ e_u\ _c$	$e_{q,l}$	$e_{qx,r}$	$\ e_q\ _*$	$\ e_q\ _c$
8	5.43e-04	7.10e-04	1.71e-04	7.45e-05	7.10e-04	1.93e-03	1.24e-04	1.71e-04
16	2.49e-05	3.44e-05	4.66e-06	2.41e-06	3.44e-05	9.91e-05	3.80e-06	4.80e-06
32	1.41e-06	1.17e-06	1.23e-07	7.30e-08	1.17e-06	4.83e-06	9.86e-08	1.31e-07
64	8.66e-08	9.71e-08	4.00e-09	2.22e-09	9.71e-08	3.76e-07	3.41e-09	4.16e-09
128	5.37e-09	5.68e-09	1.21e-10	6.81e-11	5.68e-09	3.48e-08	1.95e-10	1.25e-10
256	3.35e-10	3.35e-10	3.74e-12	2.11e-12	3.35e-10	9.06e-10	3.24e-12	3.85e-12

Table 2: Various errors for  $k=3$ .

N	$e_{u,r}$	$e_{ux,l}$	$\ e_u\ _*$	$\ e_u\ _c$	$e_{q,l}$	$e_{qx,r}$	$\ e_q\ _*$	$\ e_q\ _c$
8	1.20e-05	1.05e-05	9.51e-08	3.29e-07	1.05e-05	1.19e-05	4.22e-07	1.81e-07
16	3.42e-07	3.38e-07	5.21e-10	2.49e-09	3.38e-07	3.21e-07	2.45e-09	1.15e-09
32	1.07e-08	1.07e-08	3.50e-12	1.93e-11	1.07e-08	1.05e-08	1.92e-11	8.27e-12
64	3.35e-10	3.35e-10	2.55e-14	1.50e-13	3.35e-10	3.48e-10	1.88e-13	6.47e-14
128	1.05e-11	1.05e-11	2.00e-16	1.17e-15	1.05e-11	1.04e-11	1.25e-15	4.97e-16
256	3.27e-13	3.27e-13	1.54e-18	9.15e-18	3.27e-13	3.30e-13	1.31e-17	3.86e-18

Table 3: Various errors for  $k=4$ .

N	$e_{u,r}$	$e_{ux,l}$	$\ e_u\ _*$	$\ e_u\ _c$	$e_{q,l}$	$e_{qx,r}$	$\ e_q\ _*$	$\ e_q\ _c$
8	3.28e-07	3.60e-07	3.16e-09	2.16e-09	3.60e-07	3.58e-07	2.86e-09	2.51e-09
16	5.45e-09	5.47e-09	6.21e-12	4.70e-12	5.47e-09	5.59e-09	6.13e-12	5.09e-12
32	8.63e-11	8.64e-11	1.25e-14	9.72e-15	8.64e-11	8.68e-11	1.26e-14	1.05e-14
64	1.35e-12	1.35e-12	2.49e-17	1.95e-17	1.35e-12	1.35e-12	5.32e-17	2.16e-17
128	2.11e-14	2.11e-14	4.95e-20	3.85e-20	2.11e-14	2.11e-14	4.84e-20	4.37e-20

for  $k=3,4$  are given in Tables 4-5. We can hardly observe the desired superconvergence phenomenon for all the four errors in Theorems 3.2-3.4.

We also consider another way of initial discretization, the Radau projection  $P_h^- u$ . Numerical data are given in Tables 6-7. It seems that the convergence rate of function value approximation at the right Radau points and derivative approximation at the interior left Radau points for the variable  $u$  is  $k+2$  and  $k+1$ , respectively. However, we do not see the same convergent rates for the variable  $q$ . Moreover, we do not observe the  $(2k+1)$ -th superconvergence rate at nodes and for the cell average in both variables  $u$  and  $q$ .

The numerical comparison of initial discretization with the  $L^2$ -projection and the Radau projection indicates that the proposed correction scheme for the initial condition is necessary in order to achieve the best possible superconvergent rate in our theory.

Table 4: Various errors for  $k=3$  with initial solutions chosen as  $L^2$ -projection.

N	$e_{u,r}$	order	$e_{ux,l}$	order	$\ e_u\ _*$	order	$\ e_u\ _c$	order
8	1.45e-04	–	1.71e-03	–	1.91e-04	–	2.21e-05	–
16	5.77e-06	4.65	1.37e-04	3.64	3.74e-06	5.67	7.45e-07	4.89
32	2.98e-07	4.28	5.25e-05	1.39	1.06e-06	1.82	4.52e-08	4.05
64	2.83e-08	3.39	3.82e-06	3.78	4.75e-08	4.48	1.76e-09	4.68
128	1.33e-09	4.41	4.50e-07	3.09	2.48e-09	4.26	8.47e-11	4.38
256	1.75e-10	2.92	6.35e-08	2.82	1.03e-10	4.59	4.06e-12	4.38
N	$e_{q,l}$	order	$e_{qx,r}$	order	$\ e_q\ _*$	order	$\ e_q\ _c$	order
8	1.71e-03	–	6.24e-02	–	4.76e-03	–	2.07e-04	–
16	1.37e-04	3.64	9.22e-03	2.76	1.96e-04	4.60	1.16e-05	4.16
32	5.25e-05	1.39	3.40e-03	1.44	7.74e-05	1.34	1.88e-06	2.63
64	3.82e-06	3.78	5.86e-04	2.54	5.81e-06	3.74	1.23e-07	3.93
128	4.50e-07	3.09	1.38e-04	2.09	8.09e-07	2.84	1.10e-08	3.49
256	6.35e-08	2.85	3.59e-05	1.94	6.86e-08	3.60	1.04e-09	3.41

Table 5: Various errors for  $k=4$  with initial solutions chosen as  $L^2$ -projection.

N	$e_{u,r}$	order	$e_{ux,l}$	order	$\ e_u\ _*$	order	$\ e_u\ _c$	order
8	1.50e-05	–	1.93e-04	–	8.39e-06	–	8.48e-07	–
16	4.00e-07	5.23	1.37e-05	3.82	2.34e-07	5.17	1.82e-08	5.54
32	6.43e-09	5.96	3.17e-07	5.43	4.40e-09	5.73	4.51e-10	5.33
64	4.04e-10	3.99	7.53e-08	2.07	4.00e-10	3.46	1.37e-11	5.08
128	1.10e-11	5.19	1.98e-09	5.25	3.20e-12	6.97	4.24e-13	4.98
N	$e_{q,l}$	order	$e_{qx,r}$	order	$\ e_q\ _*$	order	$\ e_q\ _c$	order
8	1.93e-04	–	1.78e-02	–	4.25e-04	–	1.09e-05	–
16	1.37e-05	3.82	1.76e-03	3.39	2.36e-05	4.17	8.76e-07	3.64
32	3.17e-07	5.43	9.49e-05	4.17	7.22e-07	5.03	2.13e-08	5.36
64	7.53e-08	2.07	2.46e-05	1.95	5.47e-08	3.72	1.89e-09	3.49
128	1.98e-09	5.25	1.03e-06	4.58	2.17e-09	4.65	5.22e-11	5.18

### 5.2 Energy conservation

**Example 2.** As the first nonlinear example, we consider the following Sine-Gordon equation

$$u_{tt} = u_{xx} + \sin(u), \quad (x,t) \in [0,2\pi] \times [0,60] \tag{5.1}$$

with the periodic boundary condition and initial conditions

$$u(x,0) = \sin(x - 2t), \quad u_t(x,0) = -6\cos(x).$$

The equation appears frequently in variety of physical applications including relativistic

Table 6: Various errors for  $k=3$  with initial solutions chosen as  $P_h^- u$ .

N	$e_{u,r}$	order	$e_{ux,l}$	order	$\ e_u\ _*$	order	$\ e_u\ _c$	order
8	2.05e-05	–	1.16e-04	–	1.62e-05	–	2.96e-06	–
16	6.44e-07	4.99	1.35e-05	3.10	2.05e-07	6.31	9.95e-08	4.89
32	2.89e-08	4.48	5.44e-07	4.64	1.06e-08	4.27	2.65e-09	5.23
64	9.44e-10	4.94	3.42e-08	3.99	3.45e-10	4.95	7.46e-11	5.15
128	1.89e-11	5.64	2.41e-09	3.83	9.32e-12	5.21	1.88e-12	5.31
256	1.07e-12	4.15	2.02e-10	3.57	2.37e-13	5.30	4.52e-14	5.38
N	$e_{q,l}$	order	$e_{qx,r}$	order	$\ e_q\ _*$	order	$\ e_q\ _c$	order
8	1.16e-04	–	2.01e-03	–	2.42e-04	–	3.38e-05	–
16	1.35e-05	3.10	2.76e-04	2.86	5.65e-06	5.42	9.63e-07	5.13
32	5.44e-07	4.64	5.55e-05	2.32	1.18e-06	2.26	7.70e-08	3.65
64	3.42e-08	3.99	5.70e-06	3.29	5.63e-08	4.39	3.79e-09	4.34
128	2.41e-09	3.83	5.26e-07	3.44	2.70e-09	4.38	1.78e-10	4.42
256	2.02e-10	3.57	9.58e-08	2.46	1.25e-10	4.43	8.57e-12	4.37

Table 7: Various errors for  $k=4$  with initial solutions chosen as  $P_h^- u$ .

N	$e_{u,r}$	order	$e_{ux,l}$	order	$\ e_u\ _*$	order	$\ e_u\ _c$	order
8	8.40e-07	–	8.37e-06	–	2.24e-07	–	4.59e-08	–
16	1.24e-08	6.08	3.61e-07	4.54	6.62e-09	5.08	6.01e-10	6.25
32	1.71e-10	6.18	4.96e-09	6.19	4.87e-11	7.08	9.28e-12	6.02
64	5.78e-12	4.88	2.86e-10	4.11	1.26e-12	5.27	1.39e-13	6.06
128	4.50e-14	7.00	6.91e-12	5.37	1.08e-14	6.86	1.85e-15	6.23
N	$e_{q,l}$	order	$e_{qx,r}$	order	$\ e_q\ _*$	order	$\ e_q\ _c$	order
8	8.37e-06	–	1.97e-04	–	7.96e-06	–	4.17e-07	–
16	3.61e-07	4.54	7.46e-06	4.72	1.54e-07	5.69	1.04e-08	5.33
32	4.96e-09	6.19	2.10e-07	5.15	4.11e-09	5.23	2.08e-10	5.64
64	2.86e-10	4.11	6.37e-08	1.72	3.47e-10	3.56	7.09e-12	4.87
128	6.91e-12	5.37	1.50e-09	5.41	2.73e-12	6.99	2.06e-13	5.10

field theory, mechanical transmission lines, and Josephson junctions. The equation has the continuous conserved energy

$$E(t) = \int_{\Omega} \left( \frac{1}{2} u_t^2 + \frac{1}{2} u_x^2 + \cos(u) \right) dx$$

for all time. Here we set the space step-size  $h = \pi/10$ , time step-size  $\Delta t = 0.01$ , and solve the problem with our proposed method (4.1), the classical method (4.7), and the third order TVD Runge-Kutta DG method, respectively. The errors between the continuous

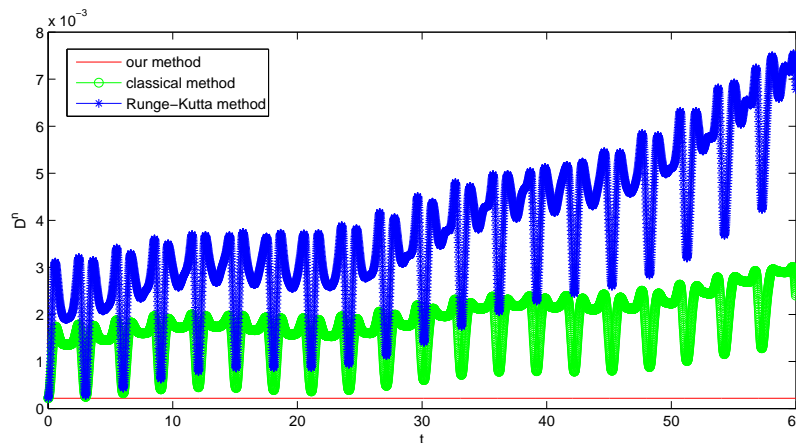


Figure 4: The errors of energy for problem (5.1).

and discrete energy are displayed in Fig. 4, where

$$D^n := |E_h^n - E(0)|.$$

Here  $E_h^n$ , defined in Theorem 4.2, is obtained by different methods. We observe that energy errors of the classical method (4.7) and the third-order TVD Runge-Kutta DG method increase almost linearly with respect to time, while the energy error from our method remains the same.

**Example 3.** As the second nonlinear example, we consider the following Klein-Gordon equation

$$u_{tt} = u_{xx} + u - u^3. \quad (x, t) \in [0, 2\pi] \times [0, T] \tag{5.2}$$

with the periodic boundary condition and the following initial conditions

$$u(x, 0) = \cos(x), \quad u_t(x, 0) = 10\text{sech}(x).$$

The equation was first considered by Schrödinger as a quantum wave equation, which was used to describe the de Broglie waves or to study the hydrogen atom. As is well-known, the equation has the continuous conserved energy

$$E(t) = \int_{\Omega} \left( \frac{1}{2}u_t^2 + \frac{1}{2}u_x^2 - \frac{1}{2}u^2 + \frac{1}{4}u^4 \right) dx$$

for all time.

In this numerical experiment, we show further that the energy conserving property of the numerical solution is due to the special treatment of the nonlinear term. Again, we set the space step-size  $h = \pi/10$ , time step-size  $\Delta t = 0.01$ . We solve the problem on the time interval  $[0, 200]$ . Fig. 5 depicts errors between the continuous and discrete energy. Again, we see that the energy errors of the proposed methods (4.1) and (4.2) remain unchanged, while the energy error of the classical method (4.7) increases linearly with time.

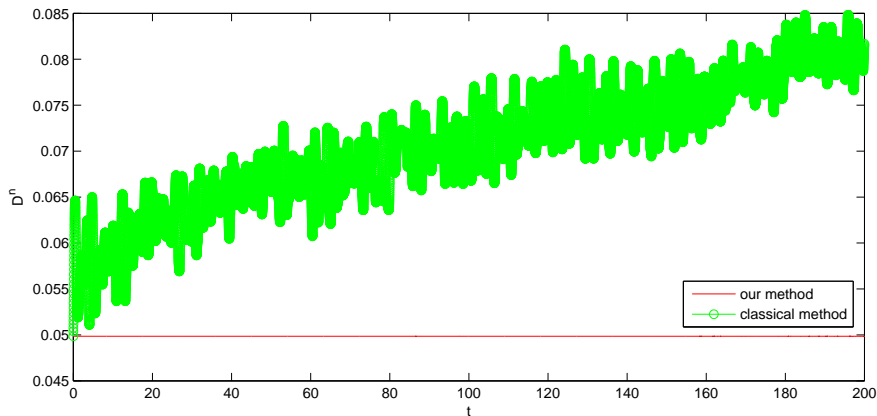


Figure 5: The errors of energy for problem (5.2).

## 6 Conclusions

Superconvergence properties of the LDG method for linear wave equations in one space dimension are studied under suitable initial discretization. We prove that, for fluxes choice (2.4), the LDG solution  $(u_h, q_h)$  is  $(k+2)$ -th order superconvergent to the Gauss-Radau projection  $(P_h^- u, P_h^+ q)$ ; the function value error  $u - u_h$  at right Radau points and  $q - q_h$  at left Radau points, converge with the same rate  $k+2$ ; the nodal errors of  $u - u_h$  at downwind points and  $q - q_h$  at upwind points, as well as their cell averages, all converge with the same rate  $2k+1$ . We prove the similar superconvergence results for fluxes choice (2.5). A surprising numerical observation is the  $(k+2)$ -th order derivative error  $\partial_x(u - u_h)$  at interior left Radau points and  $\partial_x(q - q_h)$  at interior right Radau points. Theoretical explanation of this ultra-convergence (two-orders higher than the best possible global rate) phenomenon is one of our on-going projects.

In addition, a fully discrete numerical scheme is proposed to achieve the goals of explicit time marching and energy conservation for a class of nonlinear wave equations. We prove that our algorithm preserves the discrete energy. Numerical experiments on the Klein-Gordon and Sine-Gordon equations demonstrate that our method not only preserves the energy, but also provides good approximations to the continuous solutions.

## Acknowledgments

This work is supported in part by the National Natural Science Foundation of China (NSFC) under grants Nos. 11201161, 11471031, 11501026, 91430216, U1530401, China Postdoctoral Science Foundation under grant Nos. 2015M570026, 2016T90027 and the US National Science Foundation (NSF) through grant DMS-1419040.

## References

- [1] S. Adjerid and T. C. Massey, Superconvergence of discontinuous Galerkin solutions for a nonlinear scalar hyperbolic problem, *Comput. Methods Appl. Mech. Engrg.*, 195 (2006), pp. 3331–3346.
- [2] S. Adjerid and T. Weinhart, Discontinuous Galerkin error estimation for linear symmetric hyperbolic systems, *Comput. Methods Appl. Mech. Engrg.*, 198 (2009), pp. 3113–3129.
- [3] S. Adjerid and T. Weinhart, Discontinuous Galerkin error estimation for linear symmetrizable hyperbolic systems, *Math. Comp.*, 80 (2011), pp. 1335–1367.
- [4] M. Anderson and J.H. Kimn, A numerical approach to space-time finite elements for the wave equation, *J. Comput. Phys.*, 226 (2007), pp. 466–476.
- [5] M. Baccouch, A local discontinuous Galerkin method for the second-order wave equation, *Comput. Meth. Appl. Mech. Eng.*, 212 (2012), pp. 129–143.
- [6] M. Baccouch, Superconvergence of the local discontinuous Galerkin method applied to the one-dimensional second-order wave equation, *Numer. Part. Diff. Equ.*, 30 (2013), pp. 862–901.
- [7] H. Brunner, Q. Huang and H. Xie, Discontinuous Galerkin methods for delay differential equations of pantograph type, *SIAM J. Numer. Anal.*, 48 (2010), pp. 1944–1967.
- [8] W. Cao, Z. Zhang and Q. Zou, Superconvergence of discontinuous Galerkin method for linear hyperbolic equations, *SIAM J. Numer. Anal.*, 52-5 (2014), pp. 2555–2573.
- [9] W. Cao and Z. Zhang, Superconvergence of local discontinuous Galerkin method for one-dimensional linear parabolic equations, *Math. Comp.*, 85 (2016), pp. 63-84.
- [10] W. Cao and Z. Zhang, Point-wise and cell average error estimates for the DG and LDG method for 1D hyperbolic conservation laws and parabolic equations (in Chinese), *Sci Sin Math*, 45 (2015), 1115-1132.
- [11] Y. Cheng and C.-W. Shu, Superconvergence and time evolution of discontinuous Galerkin finite element solutions, *J. Comput. Phys.*, 227 (2008), pp. 9612–9627.
- [12] Y. Cheng and C.-W. Shu, Superconvergence of discontinuous Galerkin and local discontinuous Galerkin schemes for linear hyperbolic and convection-diffusion equations in one space dimension, *SIAM J. Numer. Anal.*, 47 (2010), pp. 4044–4072.
- [13] C. Chou, C.-W. Shu and Y. Xing, Optimal energy conserving local discontinuous Galerkin methods for second-order wave equation in heterogeneous media, *J. Comp. Phys.*, 272 (2014), pp. 88–107.
- [14] E. T. Chung and B. Engquist, Optimal discontinuous Galerkin methods for wave propagation, *SIAM J. Numer. Anal.*, 44 (2006), pp. 2131–2158.
- [15] E. T. Chung and B. Engquist, Optimal discontinuous Galerkin methods for the acoustic wave equation in higher dimension, *SIAM J. Numer. Anal.*, 47 (2009), pp. 3820–3848.
- [16] M. Delfour, W. Hager and F. Trochu, Discontinuous Galerkin methods for ordinary differential equations, *Math. Comp.* 36 (1981), pp. 455–473.
- [17] D. B. Duncan, Symplectic finite difference approximations of the nonlinear Klein-Gordon equation, *SIAM J. Numer. Anal.*, 34 (1997), pp. 1742–1760.
- [18] D. A. French and T. E. Peterson, A continuous space-time finite element method for the wave equation, *Math. Comp.*, 65 (1996), pp. 491–506.
- [19] D. Furihata, Finite-difference schemes for nonlinear wave equation that inherit energy conservation property, *J. Comp. Appl. Math.*, 134 (2001), pp. 37–57.
- [20] S. Gottlieb, C.-W. Shu and E. Tadmor, Strong stability-preserving high-order time discretization methods, *SIAM Rev.*, 43 (2001), pp. 89–112.
- [21] W. Guo, X. Zhong and J. Qiu, Superconvergence of discontinuous Galerkin and local discontinuous Galerkin methods for linear hyperbolic equations, *SIAM J. Numer. Anal.*, 52-5 (2014), pp. 2555–2573.

- tinuous Galerkin methods: eigen-structure analysis based on Fourier approach, *J. Comput. Phys.*, 235 (2013), pp. 458–485.
- [22] D. Li and C. Zhang, Superconvergence of a discontinuous Galerkin method for first-order linear delay differential equations, *J. Comp. Math.*, 29 (2011), pp. 574–588.
- [23] G. Li and Y. Xu, Energy conserving Local discontinuous Galerkin methods for nonlinear Schrödinger equation with wave operator, *J. Sci. Comput.*, 2014, accepted.
- [24] Z. Xie and Z. Zhang, Uniform superconvergence analysis of the discontinuous Galerkin method for a singularly perturbed problem in 1-D, *Math. Comp.*, 79 (2010), pp. 35–45.
- [25] Y. Xing, C.-S. Chou and C.-W. Shu, Energy conserving discontinuous Galerkin methods for wave propagation problems, *Inverse Problems and Imaging*, 7 (2013), pp. 967–986.
- [26] Y. Yang and C.-W. Shu, Analysis of optimal superconvergence of discontinuous Galerkin method for linear hyperbolic equations, *SIAM J. Numer. Anal.*, 50 (2012), pp. 3110–3133.
- [27] Y. Yang and C.-W. Shu, Analysis of Sharp Superconvergence of Local Discontinuous Galerkin Method for One-Dimensional Linear Parabolic Equations, *J. Comp. Math.*, 33 (2015), pp. 323–340.
- [28] Z. Zhang, Z. Xie and Z. Zhang, Superconvergence of discontinuous Galerkin methods for convection-diffusion problems, *J. Sci. Comput.*, 41 (2009), pp. 70–93.